Applied problems of nonlinear oscillation and wave theory

Official English translation

Chaos and order in the atmosheric dynamics
Part 3. Predictability of El Niño

N. V. Vakulenko[1], *I. V. Serykh*[1], *D. M. Sonechkin*[1,2]

[1]Shirshov Institute of Oceanology, Russian Academy of Sciences
36, Nakhimovsky Prospekt, 117997 Moscow, Russia
[2]Hydrometeorological Research Centre of the Russian Federation
11–13 Bol'shoi Predtechensky per., 123242 Moscow, Russia
Email: vanava139@yandex.ru, iserykh@ocean.ru, dsonech@ocean.ru
Received 2.03.2018, accepted for publication 20.04.2018

Topic. Based on the assumption that short-term climatic variations are nonchaotic, and, therefore, the paradigm of the limited predictability of weather formulated by E.N. Lorenz is not applicable to these variations, a question is posed about the unlimited predictability of the short-term climatic variations. It differs from the opinion generally accepted in climatology now that atmospheric motions of all time scales, beginning from daily weather variations, and including interannual, centennial and even millennial variations of climate are unstable. **Aim.** Specifically, the interannual scales are considered in this paper, and the predictability of the well-known phenomenon of El Niño is investigated. For this purpose, the so-called Global Atmospheric Oscillation (GAO) is considered which has been recently recognized by climatologists. GAO represents a synchronized integrity of the well-known processes in tropics connected with El Niño, and some extratropical processes. **Method.** Assuming GAO to be the main mode of the short-term climatic variations, some indices are defined which characterize the dynamics of GAO itself as well as the interrelations between the extratropical and tropical components of GAO with each other. It turns out that crosscorrelations exist between these indices which are so high that they may be considered as evidences of some one-to-one relationships between the tropical and the extratropical components of GAO. **Results.** It allows give a positive answer to the question posed on nonchaoticity of the short-term climatic variations. Among the indices characterizing GAO there is one by means of which it is possible to predict El Niño with the lead time of 14 months. Then, by means of a specially designed technique of the crosswavelet analysis of pairs of time series, a range of time scales is found in which the closest crosscorrelations exist of the index-predictor with an index characterizing El Niño itself. This time scale range includes within itself all known El Niño rhythms, i.e. the time periods from 2 to about 16 years. **Discussion.** As a result, it is indicated a possibility of a further increase in the lead time of the of El Niño prediction up to several years. It is much more, than the lead times of all present-day hydrodynamical and statistical forecasts of El Niño.

Key words: nonchaotic short-term climatic variations, wavelet analysis, predictability of El Niño.

https://doi.org/10.18500/0869-6632-2018-26-4-75-94

Reference: Vakulenko N.V., Serykh I.V., Sonechkin D.M. Chaos and order in atmospheric dynamics. Part 3. Predictability of El Niño. *Izvestiya VUZ, Applied Nonlinear Dynamics*, 2018, vol. 26, iss. 4, pp. 75–94. https://doi.org/10.18500/0869-6632-2018-26-4-75-94

Introduction

Weather forecast has long been the main practical goal of researches in the physics of atmospheric processes. At first, such predictions were made using a great variety of empirical techniques, but in the 1930s an outstanding Soviet hydrodynamicist I.A. Kibel proposed to use hydrodynamic equations with the so-called Coriolis acceleration, considering the rotation of the Earth [1]. Previously, an American researcher L.F. Richardson [2] had already tried to use such equations for weather forecast. Unfortunately, after long calculations with an arithmometer, Richardson made a forecast for tomorrow, that turned out to be completely wrong. It was due to fast gravitational and sound waves, described by the hydrodynamic equations, that Richardson used along with weather-forming waves. The achievement of Kibel was that he modified the equations of hydrodynamics of the atmosphere, excluding from consideration the fast waves and describing only the weather-forming waves. In the Western world this achievement is associated with the name of an American researcher J. Charney [3]. However, his discoveries were made in the late 1940s, that is, a decade later than Kibel's works.

Kibel's solution became possible to apply only in the 1950s, when the first electronic computers appeared. With increase of computer power hydrodynamic models for numerical weather forecasting became more detailed. Consequently, weather forecasts were advancing rapidly. However, in the 1960s this advancement began to slow down. Meteorologists-forecasters found out that their forecasts are more or less good only for the first 24-hours of the forecast. Then the quality of forecasts began to decrease and for lead time of three to five days forecasts completely lose touch with reality. There was a suspicion that no matter how much the power of the computer increased, the detail of predictive hydrodynamic models achieved due to this could not lead to an increase in the lead time of reliable forecasts; that is, hydrodynamic forecasts have a certain, almost insuperable limit of predictability.

1. Paradigm for chaotic and limited predictability of atmospheric processes

Theoretical justification for existence of such a limit was given in a series of papers published in the 1960s by an American meteorologist and father of the chaos theory E.N. Lorenz. In his famous paper Deterministic Nonperiodic Flow [4], Lorenz developed a mathematical construction, that was later called the strange attractor. Using this construction Lorenz explained how, despite the absence of any random external influences, even an ideal hydrodynamic model of the atmosphere behaves so that even small errors in setting its initial state (those are inevitable due to incompleteness and inaccuracy of meteorological observations) have a fatal effect on the weather forecasts compiled with its help.

On the basis of this observation, Lorenz formulated the paradigm for chaoticity and limited predictability of weather-forming processes. The main mathematical cause of chaoticity is the quadratic nonlinearity of the hydrodynamic equations. From physical standpoint, this means that any fluid motion is determined by the respective pressure. But the movement itself changes this field. A changed pressure field determines the following changes in the field of motion, and so forth.

The Lorenz paradigm was later extended to longer-period atmospheric variations (climate variations). Generally speaking, there were no sufficient reasons for that. Indeed, the numerical hydrodynamic models of the long-term (for a month, for a season) weather forecasting, being developed in the USSR in the middle of the XX century by E.N. Blinova [5], were linear. Later, nonlinear models that were not fundamentally different from short-term forecasting models came into use. The output of these models was simply time-averaged, hoping that the weekly limit of the weather predictability will not affect the "climate" of these models. Unfortunately, this expectation did not come true. So far, long-term weather forecasts, as well as predictions of short-term climate variations, such as El Niño predictions, are not very successful. However, the reason for this does not seem to be the chaotic nature of climate variations.

The reason for the chaotic nature of weather variations is that very small initial condition errors in integration of predictive hydrodynamic models get larger and in about a week commensurate with the actual large-scale features of the predicted meteorological fields. Further integration becomes useless; that is, the limit of predictability is reached.

Accumulation of forecast errors is provided by the existence of an ascending cascade of energy, that is, the flow of energy directed from small to large-scale atmospheric movements. The signs of this cascade are smooth graphs of spatial and temporal power spectra for atmospheric motions with a slope approximately equal to minus two. It has long been established [6] that in the spatial spectra this cascade begins at scales of about 1000 kilometers; that is, the characteristic size of cyclones, and increases up to the planetary scale.

In temporal spectra, the cascade begins at times of about several days, that is, the characteristic lifetime of cyclones, but covers only a limited range of larger time scales. The presence of the low-frequency end in the ascending cascade of energy can be determined by transition of the spectrum graph to zero or even to a positive slope. Detailed calculations of temporal power spectra, introduced, for example, in [7], indicate that in the tropics the ascending cascade is clearly limited to the period of 45 days. Extratropical weather does not have such a distinct limit, because the slope decreases to zero very smoothly on a scale from one month to several seasons. At least, we can assume that the ascending cascade of energy does not penetrate into the interannual scales. Thus, the Lorenz paradigm is not applicable to interannual and maybe even to seasonal atmospheric variations.

It is clear that on climatic time scales (interannual and even longer), there are sources of atmospheric movement instability, that can generate their own ascending cascades of energy. For example, it may be a cascade generated by the unstable response of the Earth's climate system to the annual Sun-induced heating. In this regard, of great importance were the numerous studies, which showed that the graphs of temporal power spectra for inter-mode climatic variations are not smooth. Most of the spectral density peaks were found in the range of time scales from one year to about a decade. Especially clearly these peaks are visible in the spectra of El Niño-Southern Oscillation (ENSO) processes developing in the tropical waters Pacific ocean. The origin of these peaks has long been the subject of hot debates. Many researchers believed that these peaks, being found from fairly short series of instrumental meteorological observations, are statistically insignificant; that is, they arise "by chance" and will disappear in the course of longer observations.

There were also those who accepted the existence of peaks and associated them with some processes in the atmosphere, excited by external forces. Among these researchers, it is necessary to mention N.S. Sidorenkov who considers that the occurrence of peaks in the spectra of the ENSO processes is due to Earth's irregular rotation [8]. A similar opinion has long been held by some Western scientists.

Sidorenkov's point of view was subject to verification in [9] on the currently available and carefully verified series of instrumental meteorological observations and their so-called re-analyses, that is, series of observations, where gaps and internal inconsistencies were excluded by present-day hydrodynamic models of atmospheric and oceanic circulation. As a result, all the main peaks of the spectral density in the range of time scales from one year to decade were correlated with three external periodic forces of the climate system: the Chandler wobble in the Earth's pole motion; the Luni-Solar nutation of the Earth's axis; the solar cycle. The main periods of these forces are approximately 1.2, 18.6 and 11.5 years, respectively. They are incommensurate with each other and affect the climate system as though irrelevantly; instead of chaos they generate very complicated, seemingly random, but actually predictable variations, including the "rhythms" of the ENSO.

Since the above mentioned periods are indeed incommensurable, it is appropriate to test the hypothesis that the mathematical way of short-period climate variations is a strange nonchaotic attractor (SNA) recognized by mathematicians at the end of the XX century in solutions of simple nonlinear dynamical systems excited by two external forces, their periods being "very incommensurable" (usually in the ratio of the Golden mean $(\sqrt{5}-1)/2$). The SNA hypothesis is rather attractive because it allows predicting the future behavior of the considered dynamical system without any restrictions, at least theoretically.

The analysis conducted in [9] (see also [10, 11]) showed that the peaks in the ENSO spectra, and even in the spectra of some meteorological processes developing in the Earth's extratropical latitudes, do indeed have a characteristic of the SNA dynamics spectra. This characteristic is that the logarithm values of the peak amplitudes are connected by a linear dependence with the logarithm values of these peaks' order numbers.

The purpose of this paper is to demonstrate that, due to the SNA-nature of interannual climatic variations, El Niño can be predicted more than a year ahead of time. It surpasses the predictability limits of all existing methods of the El-Niño prediction.

2. Planetary in-phase condition of interannual atmospheric rhythms

The reason for the possibility of an unlimited El Niño prediction is that ENSO processes are not an isolated regional phenomenon. In [11] it was proved that ENSO is a part of some global process, called for this reason the Global Atmospheric Oscillation (GAO). The spatial structure of GAO was defined as a mean difference between the monthly mean fields of sea-level pressure and surface temperature in El Niño events and the events of La Niña opposite to them. For the sea level pressure field, this structure is shown in Fig. 1. It is determined by the presence of two very large areas of pressure differences of the same sign.

First, it is an x-shaped structure with a crossline that falls on the canonical area of the El Niño emergence in the Eastern Equatorial Pacific. Inside this structure, the pressure difference is negative. This means that the surface pressure inside this region is lower

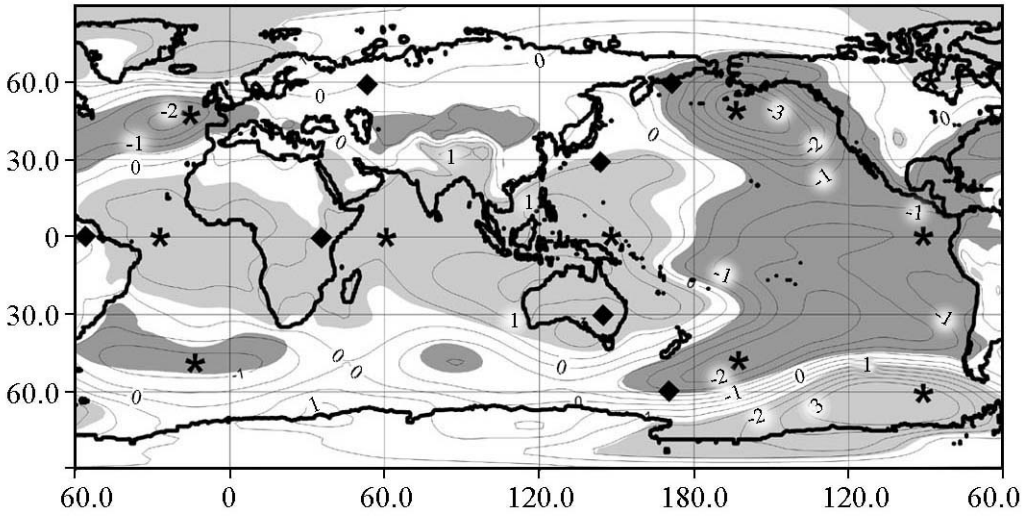

Fig. 1. The global map showing the spatial structure of the Global Atmospheric Oscillation (GAO) in the monthly mean field of the sea-level pressure (SLP, hPa) according to an analysis of instrumental meteorological observations HadSLP2 from 1920 for 2016. Symbols $*$ specify geographical areas, values of SLP in which are used to calculate the GAO1 and GAO2 indices (excepting an area on the equator near the west coast of Central America, and an area to the west from Indonesia). Symbols ♦ specify such areas used to calculate the GAO3 index

at El Niño than at La Niña. The four branches extend from the crossline towards the Bering Strait and further to the north-east of Asia, towards New Zealand, further south into the Indian Ocean, towards the south of North America and further into the North Atlantic, and finally towards the south of South America and further into the South Atlantic. Second, it is an ellipse-shaped area wherein the pressure difference is positive. It covers the Western Pacific, Australia, most of the Indian Ocean, the Equatorial Africa and the Atlantic Ocean.

It should be emphasized that both described areas are quite symmetrically located in relation to the equator. This is so despite the highly differing configuration of continents in the Northern and Southern Hemispheres exists, that would lead to different geographical localization of large-scale features for meteorological fields. The presence of the symmetry indicates that there is something more significant than the topography of the Earth's surface. It can be assumed that external forces of the climate system are common for both hemispheres. Such as the three previously mentioned forces (the Chandler wobble in the Earth's pole motion and others).

GAO can be characterized by just one number – index GAO1, that is calculated as the sum of the normalized values of sea-level pressure in ten geographical areas coinciding with extremes (maximum and minimum) in the GAO field. Setting these ten values allows us to define both of the above areas in the GAO field rather well. District centers are marked in Fig. 1 with asterisks: GAO1$= P(5°\mathrm{S}-5°\mathrm{N}, 35°-25°\mathrm{W})+P(5°\mathrm{S}-5°\mathrm{N}, 55°-$ $-65°\mathrm{E})+P(55°-65°\mathrm{N}, 95°-85°\mathrm{W})+P(65°-55°\mathrm{S}, 95°-85°\mathrm{W})+P(5°\mathrm{S}-5°\mathrm{N},$ $145°-155°\mathrm{E})-P(45°-55°\mathrm{N}, 175°-165°\mathrm{W})-P(45°-55°\mathrm{N}, 15°-5°\mathrm{W})-$ $-P(55°-45°\mathrm{S}, 15°-5°\mathrm{W})-P(55°-45°\mathrm{S}, 175°-165°\mathrm{W})-P(5°\mathrm{S}-5°\mathrm{N}, 95°-85°\mathrm{W})$. During El Niño the index is positive and during La Niña it is negative.

Two of the selected areas are canonical parts of the ENSO processes. These areas have the following coordinates (5°S – 5°N, 145°–155°E) and (5°S –5°N, 95°– 85°W).

The sea-level pressure in these areas is very different during El Niño and La Niña. Therefore, it may seem that they determine the value of the GAO1 index. If it was the case, then GAO would be nothing more than an ENSO index that is different from the previously proposed indices.

Indeed, if we calculate the ENSO index (we call it the Extended Oceanic Niño Index, EONI) as the mean seasurface temperature in the near-equatorial Pacific (5°S – 5°N, 170° – 80°W), then the crosscorrelation between the temporal variations GAO1 and EONI indices is the maximal at zero phase shift between these variations; that is, the variations occur synchronously. The value of this maximum crosscorrelation for interannual variations is very high (about 0.9). Given that the original meteorological data for the re-analysis by NOAA CIRES 20^{th} Century Global Reanalysis Version 2c, that was used for calculating this crosscorrelation, contains a large amount of observation errors, reducing any possible connection between the considered indices, we can conclude that at interannual periods there is actually a one-to-one (functional) relationship between GAO and ENSO. Besides the re-analysis, we have also investigated the observations by Met Office Hadley Center's HadSLP2 and HadCRUT.4.6 and those have demonstrated a similar result.

To ensure that the GAO and ENSO processes are not identical, we define another GAO index, further designated as GAO2. This index differs from GAO1 in that while calculating it the areas with coordinates (5°S – 5°N, 145° – 155°E) and (5°S – 5°N, 95° – 85°E), that belong to the canonical area of the Southern Oscillation, are excluded from consideration. Synchronous crosscorrelation between the GAO2 and EONI indices is also very high (approximately 0.8), although it is less than between the GAO1 and EONI indices.

The wavelet transform (WT) of EONI and GAO2 time series allows to find out which time scales variations determine this large crosscorrelation. The series and patterns of the real WT components for both series are shown in Fig. 2. Even a simple visual comparison of these patterns allows one to see that similarity between the series in the arrangement of areas where the real WT component is either positive or negative occurs only on relatively small time scales (less than about 8 years). On a scale of more than 16 years there are no similarities at all, as it seems. Note that the lack of similarity on a large scale may be due to finite length of the time series under consideration. As a result, in the WT of these series arise distortions, that are the more significant the larger the WT scale is. Indeed, to reduce this edge effect, the time series were first centered and normalized, and then at both edges supplemented with "buffers", that is, with artificial series of EONI and GAO2 constant values for 50 years. The constant values were determined by 50-year segments at the beginning and end of the actual series. However, all this does not guarantee a complete elimination of edge effect.

To evaluate the similarity degree of WT patterns on a relatively small scale with greater detail, it is convenient to consider the WT crosscorrelation pattern of the GAO2 and EONI series, shown in Fig. 3. The way it is calculated is described in the Appendix.

One can see in Fig. 3 that on time scales of less than 8 years, gray areas that correspond to in-phase variations of GAO2 and EONI cover almost the entire pattern. In this case, most of the neighboring areas, painted in gray, are separated with a bold black line. It indicates that at these scales there is an almost complete coincidence of phases of the GAO2 and EONI variations. The very small white areas at these scales are likely to be attributed to errors in meteorological observations. These areas are most

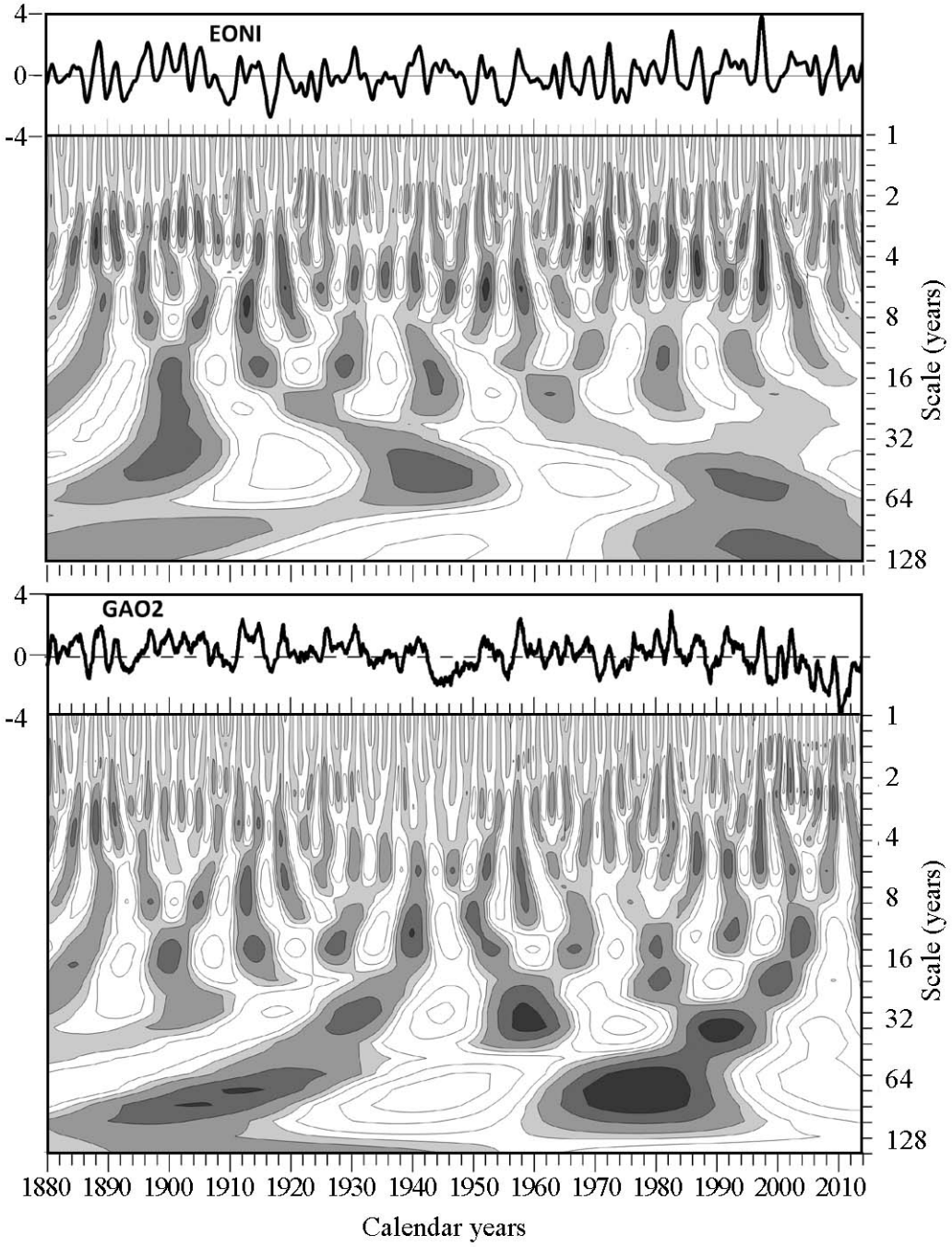

Fig. 2. Time series of EONI and GAO2 according to meteorological observations HadCRUT and HadSLP2 during 1920–2014 and patterns of the real components of the wavelet transforms of these series. Areas of positive values of real components are painted over by shades of the gray color. Areas of negative values are left white

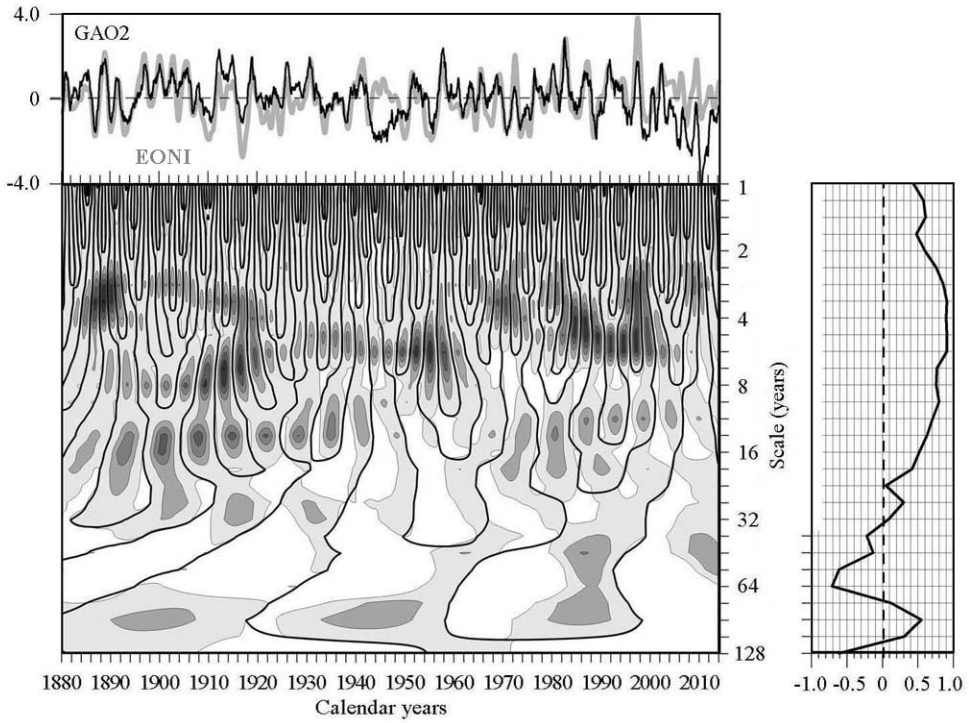

Fig. 3. Time series of GAO2 and EONI and patterns of local crosscorrelations of the real components of their wavelet transforms shown in fig. 2. Areas of positive local crosscorrelation values are painted by shades of the gray color. Areas the of the negative values are left white. Boundaries between the areas on which the real component of wavelet transform of the GAO2 series changes its sign are shown by fat black lines. Boundaries between the areas on which the sign in the EONI series changes are shown by thin black lines. To the right of the pattern, temporal mean crosscorrelations between variations in the GAO2 and EONI series are shown for each wavelet scale taken separately

noticeable in the 1930–1940s, when, due to World War II, the number and quality of observations decreased dramatically.

Gray areas also predominate at time scales from 8 to 16 years. But on the scale of more than 16 years, especially in the middle part of the pattern, that is, in the 1930–1970s, white areas predominate. On a scale of more than 32 years, the dominance of white areas exists all the time (from 1880 to 2012). However, around the scale of 64 years in the 1880–1950s, there are only white areas separated by bold lines. This may be indicative out of phase variations of this scale in compared time series, although the above mentioned edge effects in WT do not allow us to state this with a complete certainty. Because of the edge effects, the considerable positive and negative crosscorrelations on the scale of about 64 years are also rather questionable, which will be discussed further. However, large time scales are not very important from the point of view of El Niño prediction method development, which is the purpose of this work.

To the right of the local (relating to a particular calendar year) pattern of wavelet crosscorrelations in Fig. 3 is a graph of crosscorrelations calculated by averaging all local crosscorrelations for each time scale, which is being considered separately. It is seen that the mean crosscorrelations are very large (over 0.5) for the scale range from 1 to 16 years, reaching 0.9 for scales from about 3.5 to 5.6 years. As mentioned earlier, this range has the main peaks in the power spectra of GAO and ENSO attributable to the subharmonics of the Chandler wobble in the Earth's pole motion and superharmonic cycle of sunspots.

In another time scale corresponding to the superharmonics 1:2 Lunar-Solar nutation for 9.3 years, the mean crosscorrelation exceeds 0.8. The mean crosscorrelation remains quite large (about 0.5) at the scale of 16–18 years, although the spectra at these scales no longer show any peak of spectral density. These scales correspond to the main period of Lunar-Solar nutation (18.6 years) that is too large to estimate its spectral density in series of only about 100 years. However, significant mean crosscorrelations during this period are probably real. If only because the two most powerful El Niño in the history of instrumental meteorological observations (1997–1998 and 2015–2016) are separated exactly by this period.

At even larger time scales, mean crosscorrelations decrease dramatically, sometimes they even become negative. Indeed, averaging of wavelet crosscorrelations at these scales is extremely unreliable, because less than a dozen variations of such scales fit the entire range of observations. But, in any case, the large areas of local crosscorrelations visible at these scales, as already mentioned above, are almost all white; that is, they correspond to the antiphase of the compared GAO2 and EONI variations. From the above we can conclude that the extratropical component dynamics of the GAO and EONI (ENSO) is not identical. There is a great deal of similarity between these processes in the time scale range from about a year to a decade, but the behavior of GAO and EONI (ENSO) over several decades is quite different.

Hitherto, it has been a common practice to interpret the existence of strong crosscorrelations between various ENSO indices and extratropical indices of the atmospheric processes in such a way, that ENSO was considered the cause, and extratropical processes – it's consequences. However, many years ago A.N. Kolmogorov warned about the wrongness of interpreting crosscorrelation links between different time series in terms of causes and consequences. Subsequently, the problem of phase synchronization of coupled nonlinear oscillators was considered by many researchers. Let us point to Blekhman's book [12], to a relatively recent British publication [13], and also to a recent journal publication in SCIENCE [14], that provides excellent illustrations of the difficulties encountered in the study of cause-effect relationships in nonlinear systems.

In considering the problem of the relationship between ENSO processes and extratropical processes in the global climate system, it is natural to assume that there is a forced phase synchronization when both subsystems are under the influence of the same periodic external forces. Such synchronization differs from the often considered internal synchronization of nonlinear oscillators connected with each other (known Huygens principle). Indeed, the ENSO processes somehow do interact with extratropical processes. However, these interactions are still very poorly understood. Probably, they manifest themselves through the whole chain of interactions. For instance, the influence of El Niño on processes in the North Atlantic or, conversely, the influence of the North Atlantic on El Niño cannot be direct.

3. Predictability of El Niño

As mentioned above, one of the most important external forces of the climate system is probably the Chandler wobble in the Earth's pole motion. As it was determined in the second half of the XX century [15, 16], this wobble excites tidal waves in the atmosphere and oceans, propogating from West to East in out-of-phase throughout the extra-tropical

latitudes of both Hemispheres. These waves are called “pole tides”. Recently, by analyzing satellite altimetry data of the Pacific Ocean surface, it was shown [17] that the wave of the North Pacific pole tide, after reflecting from the Western coast of North America, excites a warm surface current in the subequatorial Pacific Ocean. These are just positive temperature anomalies called El Niño, that is a constituent element of ENSO.

As for the polar tides in the atmosphere, they also propogate from West to East, but the continents are not an insurmountable obstacle for them. Therefore, we can expect that the West-East propogation will also be observed in the GAO dynamics. When considering temporal changes in the GAO spatial structure in the sea-level fields, such a propogation was indeed found. It turned out that during this propogation both previously mentioned spatial areas in the GAO field are shifted from West to East and move into each other; that is, the x-shaped region after moving over the continent of America and the Atlantic becomes elliptical, and the elliptical area becomes x-shaped after its center moves to the West of the Pacific. Both transformations occur approximately 14 months before the next El Niño event. At this time the general pattern of the GAO field can be characterized by one number – another GAO index, that we call GAO3. GAO3 is calculated as the sum of the normalized values of monthly mean surface pressure in 7 geographical areas: GAO3 = P(50°N – 70°N, 170°E – 120°W) + P(70°S – 50°S, 170°E – 120°W) + +P(60°S – 20°N, 40°E – 80°E) + P(30°S – 30°N, 70°W – 10°W) – P(0°– 40°N, 120°E – 120°W) – P(45°S – 25°S, 120°E – 60°W) – P(50°N – 70°N, 50°E – 90°E). The centers of all seven areas are marked in Fig. 1 with diamonds.

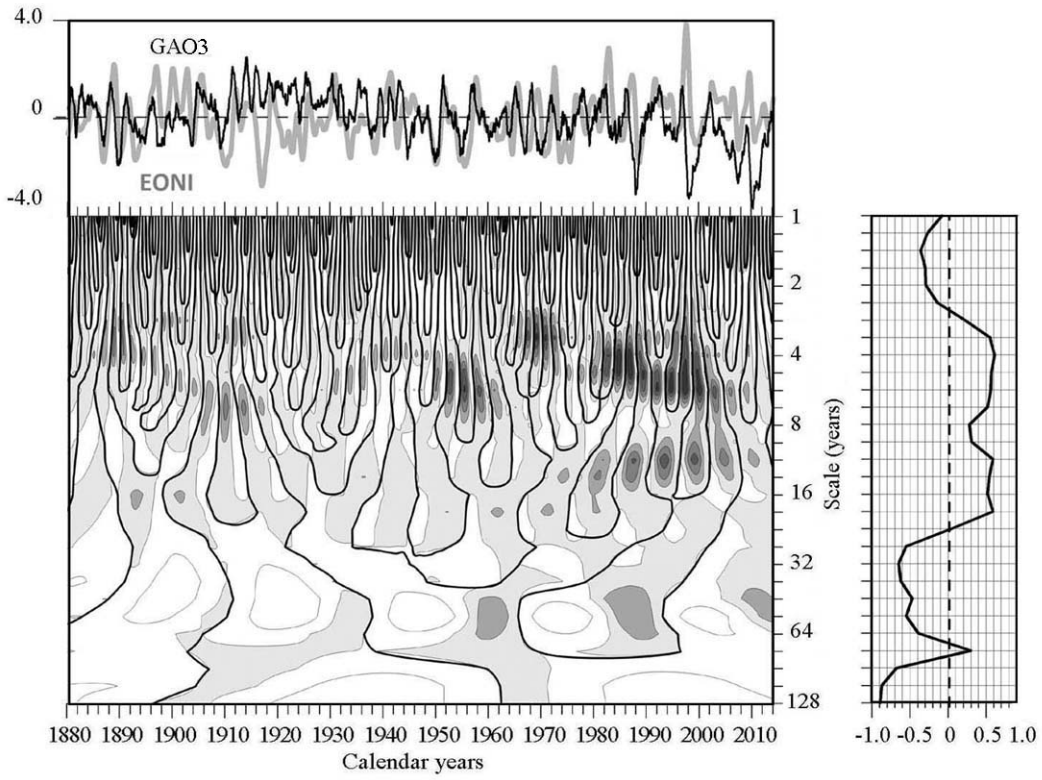

Fig. 4. The same is shown that in fig. 3, but for the GAO3 and EONI series. The pattern of the real component of the GAO3 wavelet transform is displaced for 14 months ahead

A time series of GAO3 index values was constructed. This series is shown at the top of the figure 4 together with EONI series. Both series are centered and normalized. One can see that the main extrema of GAO3 series are lead extrema of EONI series for about a year. So it seems that GAO3 can be used to predict EONI, that is, whether El Niño or La Niña will be observed with about a year in advance.

To evaluate this possibility more definitely, we have calculated the crosscorrelations between these series at different time scales and with different time shifts between these series. For this purpose we have specially designed a technique of the crosswavelet analysis for pairs of time series, as described in the Appendix. The picture of local wavelet crosscorrelations, that is, relationships between variations in these series at each wavelet (time) scale and for each calendar year, is shown in Fig. 4. GAO3 series is already shifted forward in time for the period of 14 months. To the right of this pattern, the averages of these local wavelet crosscorrelations for all time scales are shown separately.

It can be seen that the upper half of the picture, starting with a time scale of 2 years and up to a scale between 16 and 32 years, is dominated by areas marked in shades of gray. The mean local crosscorrelations at these scales exceed 0.5 (except for the time scale of about 8 years).

Thus, the relationships between anticipatory GAO3 variations and subsequent EONI variations at these scales are not much smaller than the same dependencies between synchronous GAO2 and EONI variations shown in Fig. 3. Hence, they can be used for forecasting purposes. Note that the current forecasts of El Niño / La Niña have a crosscorrelation with the facts at the level of 0.5 only with lead time of about half a year, not 14 months, as in the case of GAO3. On the time scales larger than luni-solar nutation (18.6 years), the relations between shifted forward GAO3 and EONI become, in general, nonsynchronous. Therefore, they can no longer be used for predictive purposes.

It is easier to look at the patterns of synchronous and nonsynchronous crosscorrelations between the WT series of GAO3 and EONI as shown in Fig. 5 for calendar years 1960–2014. During these years, meteorological observations were the most complete and accurate compared to the previous observation period. At the top of Fig. 5 one can see again the segments of the original GAO3 and EONI series. They clearly show that almost all the EONI maxima and minima are late compared to the GAO3 maxima and minima for about one year, and sometimes even more.

The upper of shown in Fig. 5 patterns of local wavelet crosscorrelation between the GAO3 and EONI series corresponds to zero time-shift between the compared series; the middle pattern corresponds to the time-shift of GAO3 series time-shift for 14 months forward, as well as the pattern of crosscorrelation between the WT GAO3 and EONI full series is shown in Fig. 4; the bottom picture is a time shift of as much as 38 months. In the last pattern the WT sign of the shifted GAO3 series was changed to the opposite.

Zooming of patterns in Fig. 5 compared with the pattern in Fig. 4 allows one to clearly see that in the range of time scales from 4 to about 5.7 years and from 8 to 16 years, after almost all bold black lines (let us recall that they indicate a change of the real component sign in WT GAO3 series) there are white areas. Comparing these white areas with the graphs of GAO3 and EONI series, one can see that they correspond to the periods of time when the value of GAO3 has already started to decrease, and the value of EONI is still growing. These white areas occupy about half of the distance (in calendar years) to the next bold black line. The second half of these distances is separated

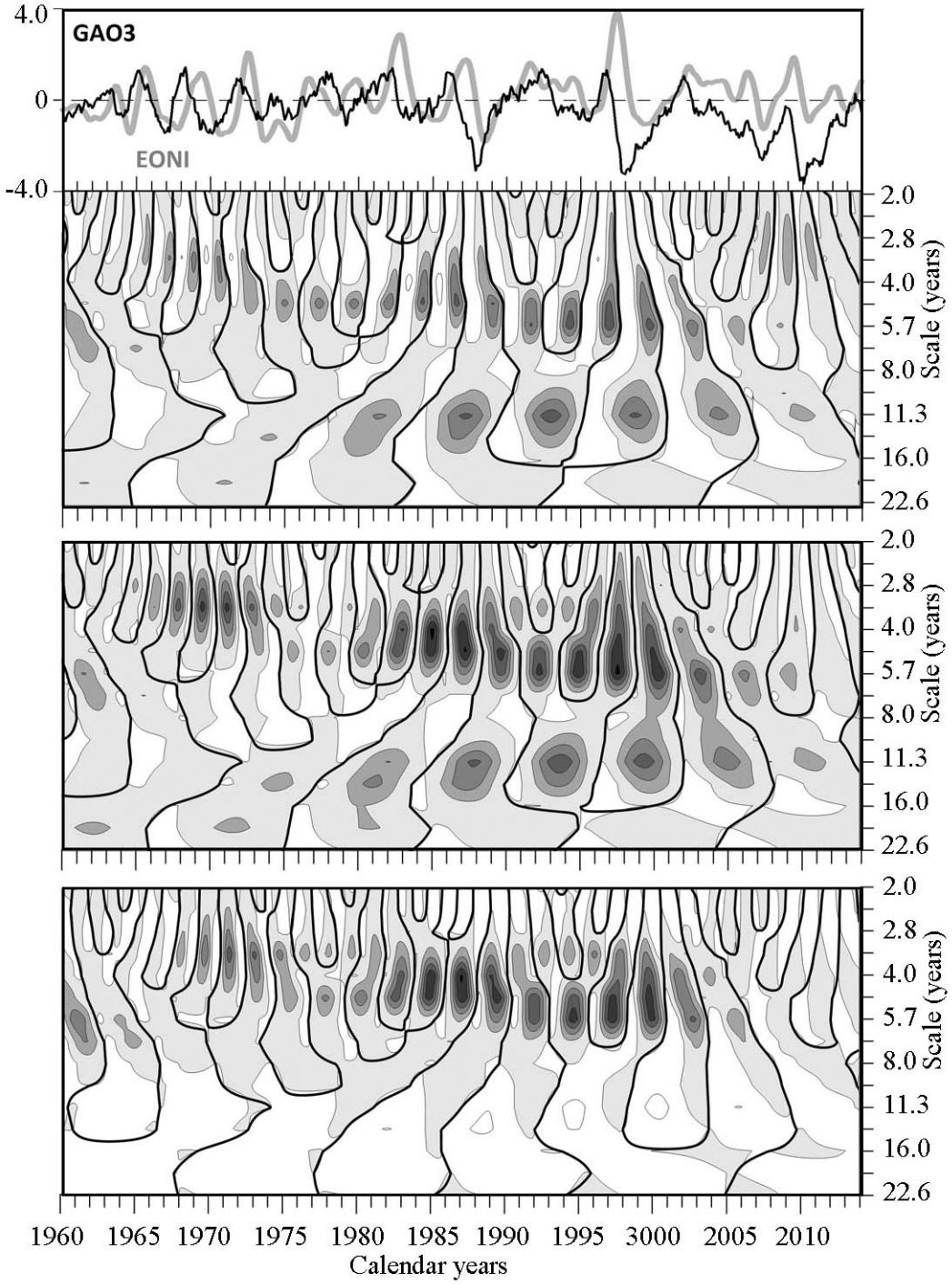

Fig. 5. The same is shown that in fig. 4, but only for an interval of calendar years 1960–2014 in the absence of temporary displacement of a row GAO3 (the top pattern), at the displacement of 14 months (an average pattern) and at the displacement of 38 months, and the signs of the real component pattern of the GAO3 wavelet transform are changed to the opposite signs (the lower pattern)

from the first half by thin black lines. It means that at time corresponding to these thin lines the real component sign in the WT EONI series is changing, and the sign of the GAO3 series remains unchanged, so that in these periods of time the values of both real components in GAO3 and EONI series simultaneously decrease.

Turning now to the picture of WT crosscorrelations in GAO3 and EONI series, shown for a time-shift of 14 months, we see a qualitative change in the fact that in both of the above areas of time scales, there are only gray areas separated by bold black lines. It means that the variations of the real components in both series at these scales were completely in-phase. In other words, the predictions for real component values in EONI series according to value of such components in GAO3 series taken 14 months earlier would be quite successful. In particular, on graphs of GAO3 and EONI series shown at the top of Fig. 5, and the corresponding section of the WT pattern for GAO3 series shift for 14 months it can be seen that prediction of the strongest El Niño (1997) would have been successful. The only exception is the range of calendar years 1970–1980 with white areas. These predictions would have been unsuccessful.

After this article was prepared, there occurred a new powerful El Niño in 2015. All the current prognostic schemes gave false alarm about the beginning of this El Niño in 2014 and only then corrected their predictions with small lead time. An additional calculation of the GAO3 index showed that El Niño 2015–2016 could have been predicted with a lead time of 14 months, although its power, of course, would have been underestimated, as it is typical of all prognostic schemes based on linear regression.

Finally, let us consider the pattern of local WT crosscorrelations of GAO3 and EONI series calculated for a time shift of 38 months. One can see that the range of time scales from 2.8 to 5.7 years is characterized by a dominance of grey areas separated by bold black lines. Although in many cases white stripes can be seen (they are particularly narrow in the 1970–2007 calendar year interval), it might be said that variations of these scales in the EONI series can indeed be quite well predicted based on variations in GAO3 series with a lead time of 38 months with the sign of these latter variations being reversed.

On the other hand, in the range of time scales from 8 to 16 years dominate the white areas, outlined on the left with bold black lines and then passing (through thin black lines) into the gray area. This indicates that predictions with a lead time of 38 months for a given range of time scales are rather difficult.

4. Conclusion

The generally accepted paradigm of limited predictability of weather and climate variations has been revised. For this purpose, the idea of a strange non-chaotic nature of short-term climate variations, previously obtained by analyzing the temporal power spectra in a series of meteorological observations, is used.

The main mode of short-term climate variations is the recently revealed so-called Global Atmospheric Oscillation (GAO) that includes, as a component part, the processes of El Niño-Southern Oscillation (ENSO). We have defined the indices characterizing GAO and ENSO, among those is the GAO3 index; its temporary changes precede temporal changes of the EONI index, characterizing the ENSO processes.

Using a specially developed technique for analyzing crosscorrelations between time series, we have identified scale ranges with a close relationship between the time variations

of the GAO3 index-predictor and the EONI index. That is interannual and decadal time scales, wherein, as shown earlier, the global climate system is affected by several external forces while their periods appear to be incommensurable with each other. In addition to the annual Sun induced heating, these forces include Chandler wobble in Earth's pole motion, Lunar-Solar nutation and the cycle of solar activity. As a result, it is possible to predict the EONI index, characterizing the ENSO, with a lead time of 14 months, that significantly exceeds the current lead-time forecasts of ENSO. We have also pointed out that it is possible to increase the lead time up to several years.

Appendix

Crosscorrelation between pairs of time series by their wavelet transforms

The wavelet transform (WT)

$$WT_b(a) = a^{-1/2} \sum_{t=t_1}^{t=t_n} X(t) G(t - b/a) \tag{1}$$

is a popular technique for studying many multiscale variations in time series. In (1) $X(t)$, $t = t_1, t_2, t_3, ..., t_n$ is a transformable series, $b = t_1, t_2, ..., t_n$ are temporal shifts of this series, $a = a_1, a_2, ..., a_m$ are wavelet time scales, and $G(t - b/a)$ is a wavelet function. The output of the WT is a pattern of the $WT_b(a)$ values in a part of the half-plane (b, a), limited by the time scale of the transformed series and the range of the time scales being considered.

One of the most commonly used wavelet functions is the Morlet wavelet

$$G(t) = \pi^{-0.25} \exp(-t^2/2) \exp(i\mathrm{C}t), \quad \mathrm{C} > 5. \tag{2}$$

In this paper we use the value $\mathrm{C} = 6.2035$, wherein the wavelet time scale exactly corresponds to the usual time scale. The Morlet wavelet enables a convenient study of wavelike variations in time series, because, in addition to real component ($\mathrm{Re}\, WT_b(a)$) and imaginary component ($\mathrm{Im}\, WT_b(a)$), the amplitude $\mathrm{Am}\, WT_b(a) = \sqrt{(\mathrm{Re}\, WT_b(a))^2 + (\mathrm{Im}\, WT_b(a))^2}$ and phase $\mathrm{Ph}\, WT_b(a) = \tan^{-1}\left(\dfrac{\mathrm{Im}\, WT_b(a)}{\mathrm{Re}\, WT_b(a)}\right)$ can be used as the output product.

WT is different from the Fourier spectral analysis because it is equally applicable to the analysis of stationary and nonstationary time series. However, previously there was no WT version similar to the cross-spectral analysis. Only recently in [18–20] for this purpose it was proposed to calculate the product of real components for two considered series

$$\mathrm{Cross}\, WT_b(a) = \mathrm{Re}\, WT1_b(a) \cdot \mathrm{Re}\, WT2_b(a) \tag{3}$$

This product is a kind of local (in time and in wavelet scale) crosscorrelation of the compared series. The areas in the picture of all such products, wherein the products are positive, are painted in shades of gray, being proportional to the product. The areas wherein the products are negative are left white. The border between the gray and white areas is marked by a bold black line, if with the time growth (from left to right in the picture) the transition between the areas in the considered time scale is due to the change

of the WT sign in the first series; that is, the variations of this series in the considered time scale are lead of the corresponding variations of the second series. This border is marked with a thin black line, if the first are variations in the second series. Similarly, the bold line on the border between the white and gray areas indicates leading variations of the second series, and the thin line indicates leading of the first series. The bold line on the boundary between two adjacent gray areas indicates a complete phase synchronization of the series variations being considered, and the thin line on the boundary between adjacent white areas indicates their out-of-phase behavior.

The research was carried out partially under the financial support by the grant of Russian Science Foundation (project No. 14-50-00095).

References

1. Kibel I.F. Vvedebie v Gidrodinamitcheskie Metodi Kratkosrochnogo Prognoza Pogodi. M.: Gostechizdat, 1957. 375 s. (in Russian).
2. Richardson L.F. Weather Prediction by Numerical Process. Cambridge: Cambridge Univ. Press, 1922. 236 p.
3. Charney J. On the scale of atmospheric processes. *Geofys. Publ*., 1948, vol. 17, pp. 1–17.
4. Lorenz E.N. Deterministic nonperiodic flow. *J. Atmos.Sci.*, 1963, vol. 20, pp. 130–141.
5. Blinova E.N. Dinamika Atmosphernich Dvijeniy Planetarnogo Masshtaba i Gidrodinamicheskiy Dolgosrochniy Prognoz Pogodi. M.: Gidrometeoizdat., 1976. 78 s. (in Russian).
6. Saltzman B., Teweles S. Further statistics on the exchange of kinetic energy between harmonic components of the atmospheric flow. *Tellus*, 1964, vol. 16, pp. 432–435.
7. Serykh I.V., Sonechkin D.M. Chaos and order in atmospheric dynamics. Part 1. Chaotic weather variations. *Izvestiya VUZ, Applied Nonlinear Dynamics*, 2017, vol. 25, iss. 4, pp. 4–22. DOI:10. 18500/0869-6632-2017-25-4-4-22.
8. Sidorenkov N.S. Atmosphernie Prozessi i Vraschenie Zemli. StPb.: Gidrometeoizdat, 2002. 200 s. (in Russian).
9. Serykh I.V., Sonechkin D.M. An Intercomparison of temporal power spectra of the El Niño – Southern Oscillation indices and of the global temperature and pressure fields in the surface layer. *Fundamentalnaya I Prikladnaya Klimatologia*, 2017, vol. 2, s. 144–155 (in Russian).
10. Serykh I.V., Sonechkin D.M. Manifestations of motions of the Earth's pole in the El Niño – Southern Oscillation Rhythms. *Doklady Earth Sciences*, 2017, vol. 472, no. 2, pp. 256–259.
11. Byshev V.I., Neiman V.G., Romanov Y.A., Serykh I.V., Sonechkin D.M. Statistical significance and climatic role of the Global Atmospheric Oscillation. *Oceanology*, 2016, vol. 56, no. 2, pp. 165–171.
12. Blekhman I.I. Sinchronizaziya Dinamitcheskich System. M.: Nauka, 1971. 896 s. (in Russian).
13. Pikovsky A. Rosenblum M., Kurths J. Synchronization. A Universal Concept in Nonlinear Sciences. Cambridge: Cambridge Univ. Press, 2001. 496 p.

14. Sugihara G., May R., Ye H., Hsieh C.-H., Deyle E., Fogarty M., Munch S. Detecting causality in complex systems. *Science*, 2012, vol. 338, pp. 496–500.
15. Maximov I.V. Poljusniy priliv v moriach i atmosphere Zemli. *Trudy instituta okeanologii AN USSR*, 1955, no. 8, s. 92–118 (in Russian).
16. Bryson R.A., Starr T.B. Chandler tides in the atmosphere. *J. Atmos. Sci.*, 1975, vol. 34, pp. 1975–1986.
17. Serykh I.V., Sonechkin D.M. Confirmation of the octanic pole tide influence on El Niño. *Sovremennije problemi distanzionnogo zondirovaniya Zemli iz Kosmosa*, 2016, vol. 13, no. 2, s. 44–52 (in Russian).
18. Vakulenko N.V., Kotlyakov V.M., Sonechkin D.M. Lead–lag relationships between atmospheric trends of temperature and carbon dioxide concentrations during the Pliocene. *Doklady Earth Sciences*, 2016, vol. 467, part 2, pp. 423–426.
19. Vakulenko N.V., Kotlyakov V.M., Parrenin F., Sonechkin D.M. A study of different scale relationship between changes of the surface air temperature and the CO_2 concentration in the atmosphere. *Ice and Snow*, 2016, vol. 56(4), pp. 533–544.
20. Vakulenko N.V., Kotlyakov V.M., Sonechkin D.M. The connection between the growth of anthropogenic carbon dioxide in the atmosphere and the current climate warming. *Doklady Earth Sciences*, 2017, vol. 477, part 1, pp. 1307–1310.